Accepted Manuscript

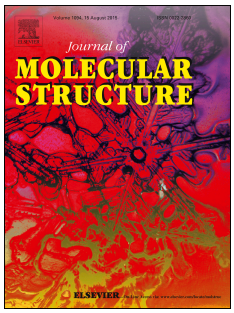

Hydrolytic degradation of *N*,*N*'-ethylenedimaleimide: Crystal structures of key intermediates and proposed mechanisms

Xue-Jie Tan, Shuang-Shuang Cheng, Yan Shi, Dian-Xiang Xing, Yun Liu, Hui Li, Wen-Quan Feng, Jian-Bo Yang

PII: S0022-2860(16)30686-X

DOI: 10.1016/j.molstruc.2016.07.015

Reference: MOLSTR 22718

To appear in: *Journal of Molecular Structure*

Received Date: 1 March 2016

Revised Date: 3 July 2016

Accepted Date: 8 July 2016

Please cite this article as: X.-J. Tan, S.-S. Cheng, Y. Shi, D.-X. Xing, Y. Liu, H. Li, W.-Q. Feng, J.-B. Yang, Hydrolytic degradation of *N*,*N*'-ethylenedimaleimide: Crystal structures of key intermediates and proposed mechanisms, *Journal of Molecular Structure* (2016), doi: 10.1016/j.molstruc.2016.07.015.

Graphic Abstract

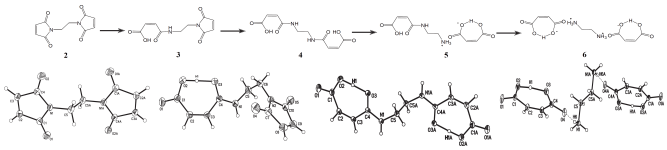

Five single-crystal structures related with the hydrolytic degradation of N,N'-ethylenedimaleimide have been investigated and the mechanisms without or with water catalysis have been proposed.

Hydrolytic degradation of N,N'-ethylenedimaleimide: crystal structures of key intermediates and proposed mechanisms

Xue-Jie Tan *, Shuang-Shuang Cheng, Yan Shi, Dian-Xiang Xing, Yun Liu, Hui Li, Wen-Quan Feng, Jian-Bo Yang

School of Chemistry and Pharmaceutical Engineering, Qilu University of Technology, Jinan, Shandong Province, 250353, P. R. China.

Abstract

Maleimide groups are used extensively in bioconjugation reactions, but limited mechanistic studies are available regarding their hydrolysis reactions. In this paper, five single-crystal structures related with the reaction of four-step hydrolytic degradation of N, N'-ethylenedimaleimide have been investigated. On the basis of experimental results, the reaction mechanisms without or with water catalysis are proposed, which could provide some enlightenment into the study of similar hydrolytic degradations.

1. Introduction

Maleimides are an important class of substrates for biological, pharmacological and chemical applications.[**1** and the references therein] The most important aspects are its ability to react through Michael addition with nucleophilic functional groups, especially amine and thiols, as well as its propensity to undergo Diels–Alder cycloadditions, which have led to its use for site-specific biomolecule ligation and modification. [**2** and the references therein].On August 19th, 2011, brentuximab vedotin (Adcetris) received FDA approval for relapsed Hodgkin lymphoma and anaplastic large cell lymphoma,[**3**] On February 22nd, 2013, another antibody-drug conjugate (ADC) ado-trastuzumab emtansine (Kadcyla) also received FDA approval for patients with HER2+ metastatic breast cancer.[**4**] Both of these therapeutics share common structural features found in most ADCs: a thiosuccinimide linkage, formed through the reaction of thiol and alkyl maleimide functionalities[**5**]. However, it has become apparent that thiosuccinimide formation is reversible, so in the bloodstream, the variable stability of ADCs formed with traditional N-alkyl maleimides usually leads to loss of drug and the released drug may show toxicities [**6**]. The thiol–maleimide adduct undergo two competing reactions: hydrolysis of the thiosuccinimide ring and cleavage of the thioether bond. The former can greatly retard the latter and help to develop a stable formulation for ADC product [**6(b), 7**].

As is known, the hydrolysis of N-alkylmaleimide ring has two steps: the first hydrolysis product is N-alkylmaleamic acid, which can be further hydrolyzed into maleic acid with elimination of N-alkylamine. According to the results of Dahlgren [**8**], Kirby [**9**] and Matsui [**10**], the secondary hydrolysis reaction of the maleimide moiety hardly occurs under their experimental conditions (in aqueous solution over the temperature range 10-50 ℃ below pH 9). But they did not explain the reason and the mechanisms of the continual hydrolysis processes are still unclear now. More importantly, the crystal structures of the products in the two-step hydrolysis have

* Corresponding author. E-mail: tanxuejie@163.com, Tel.: +86 531 89631208; fax: +86 531 89631207.

hardly been explored.

In this paper, a symmetrical bismaleimide (N, N'-ethylenedimaleimide, **2**, **Scheme 1**) was chosen as the model to explain how these hydrolytic degradations occur. In order to have a better understanding of the degradation mechanism, we have isolated nearly all key intermediates and studied their single crystal structures.

2. Experimental

2.1. Materials and measurements

All chemicals were purchased from Aladdin-reagent Chemicals and were used without further purification. Elemental (C, H, N) analyses were carried out with a Perkin–Elmer 2400 microanalyzer. ^{1}H NMR spectra were run on a Bruker Avance 400 MHz instruments. The chemical shifts are reported in parts per million (ppm) relative to tetramethylsilane, $SiMe_4$ (δ = 0 ppm), referenced to the chemical shifts of residual solvent peak [deuterated dimethyl sulfoxide (DMSO-d6)]. Melting points were determined on a WRS-2A electrothermal digital melting point apparatus (Shanghai precision & scientific instrument Co., Ltd, China).

2.2. Synthesis and crystallization

Synthesis of unsaturated analogue of demethyl-cantharidin (**UDMC**) follows methods in the literature [**11**]. Condensation of ethanediamine (**EDA**) with **UDMC** in anhydrous toluene gave the crude product of **1**, which was filtered, washed and then recrystallized in acetonitrile. **2** was prepared by heating **1** over 120□ in DMF for 12 h, employing a reverse Diels-Alder reaction. The solvent was evaporated under reduced pressure to afford **2**, which was recrystallized in acetonitrile. Then a solution of **2** in ethanol/H_2O was refluxed for 24 h. The solvent was evaporated under reduced pressure to yield white residue. The residue was dissolved in turn with dichloromethane, methanol and water. The solvents were subsequently removed by evaporation. **3**, **4** and **6** were found in dichloromethane, methanol and water, respectively. The general reactions are shown in **Scheme 1**:

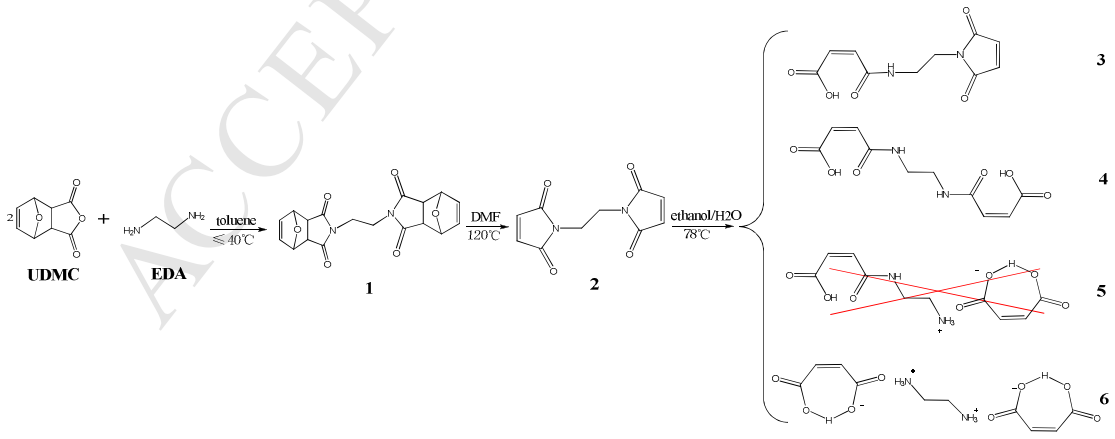

Scheme 1. the reaction sequence and hydrolysis products in this paper. Systematic names for five products: **1**, 2,2'-(1,2-ethanediyl)bis(3a,4,7,7a-te-trahydro-4,7-epoxy-1,3-bishydroisoindole-1,3-dione); **2**, N,N'-ethylenedimaleimide; **3**, 4-(N-maleimidoethyl) amino-4-oxobutenoic acid; **4**, N,N'-ethylenediamino-bis(4-oxobutenoic acid); **6**, Ethylenediammonium bis(hydrogen maleate).

Compound **5** is predicted but not obtained experimentally.

The physico-chemical characterization results are listed below:

1 Elemental analysis: found (calc. for $C_{18}H_{16}N_2O_6$): C, 60.72 (60.67%); H, 4.65 (4.53%); N, 7.98 (7.86%); HRMS (ESI): *m/z* calcd for $C_{18}H_{16}N_2O_6+H^+$: 357.1087 [$M+H^+$]; found: 357.1093; M.p.184.4-184.9℃. ^{1}HNMR (DMSO): δ (ppm) 6.510(s, 4H, olefinic protons), 5.072(s, 4H, methine protons linked to bridge O, O-CH-), 3.528(s, 4H, methylene protons, -CH_2-), 2.850(s, 4H, methine protons, -CH-). ^{13}C NMR (DMSO): δ (ppm) 175.99(carbonyl carbons), 136.38(olefinic carbons), 80.19(methine carbons linked to bridge O, O-CH-), 46.99(methine carbons, -CH-), 35.10(methylene carbons, -CH_2-). FT-TR(cm^{-1},KBr): 3098(w, ν C=C-H), 3032(w, ν C=C-H), 2993(w, ν C-H), 2957(w, ν C-H), 1770(s, ν C=O), 1720(vs, ν C=O), 1398(vs, ν C-N), 1165(s, ν C-O-C); UV/Vis (CH_3CN) λmax/nm (ε/L·mol^{-1}·cm^{-1}): 206.0(2.3×10^5).

2 Elemental analysis: found (calc. for $C_{10}H_8N_2O_4$): C, 54.52 (54.55%); H, 3.69 (3.66%); N, 12.79 (12.72%); M.p.188.7 -190.1℃. ^{1}HNMR (DMSO): δ (ppm) 6.911(s, 4H, olefinic protons), 3.726 (s, 4H, methylene protons, -CH_2-).

3 Elemental analysis: found (calc. for $C_{10}H_{10}N_2O_5$): C, 50.48 (50.42%); H, 4.31 (4.23%); N, 11.79 (11.76%); M.p.149-151℃. ^{1}HNMR (DMSO): δ (ppm) 6.815(s, 2H, olefinic protons in maleimide cycle), 6.522 (d, J=12.4 Hz, 1H, olefinic protons in maleamic acid), 6.094 (d, J=12.4 Hz, 1H, olefinic protons in maleamic acid), 3.704(m, 2H, methylene protons, -CH_2-), 3.375(m, 2H, methylene protons, -CH_2-). ^{13}C NMR (DMSO): δ (ppm) 172.22(C=O in maleimide cycle), 171.72(C=O in maleamic acid), 167.42(C=O in maleamic acid), 138.20(C=C in maleamic acid), 136.29(C=C in maleimide cycle), 132.39(C=C in maleamic acid), 51.68(-CH_2- linked to maleimide N), 37.32(-CH_2- linked to –NH-).

4 Elemental analysis: found (calc. for $C_{10}H_{12}N_2O_6$): C, 46.92 (46.88%); H, 4.70 (4.72%); N, 10.97 (10.93%); M.p.182-184℃(lit.[**12**] 197℃). ^{1}HNMR (DMSO): δ (ppm) 6.526 (d, J=12.4 Hz, 2H, olefinic protons in maleamic acid), 6.090 (d, J=12.4 Hz, 2H, olefinic protons in maleamic acid), 3.402(s, 4H, methylene protons, -CH_2-).

6 Elemental analysis: found (calc. for $C_{10}H_{16}N_2O_8$): C, 41.17 (41.10%); H, 5.56 (5.52%); N, 9.63 (9.59%); M.p.133-135℃. ^{1}HNMR (DMSO): δ (ppm) 7.671(s, 6H, -NH_3^+), 6.020 (s, 4H, olefinic protons in maleic acid), 3.921(s, 4H, methylene protons, -CH_2-). ^{13}C NMR (DMSO): δ (ppm) 167.16(C=O), 136.09(C=C), 41.00(-CH_2-).

2.3. X-Ray Crystallographic Analysis

The X-ray diffraction measurements were made on a Bruker APEX II CCD area detector diffractometer at 293/298K for compounds **1** to **6** (Mo Ka radiation, graphite monochromator, λ = 0.71073 Å). The structures were solved by SHELXL-97. The absorption correction was done using the SADABS program.[**13**] Software packages APEX II (data collection), SAINT (cell refinement and data reduction), SHELXTL (data reduction, molecular graphics and publication material), DIAMOND (simplifying crystal packing diagram) were also used.[**14**, **15**, **16**] All non-hydrogen atoms were refined with anisotropic displacement parameters. In **1**, hydrogen atoms were added to the structure model on calculated positions but in the rest four crystal structures, the positions of all hydrogen atoms

(except H9 in **3**) were experimentally determined in electron density maps and refined without any constraints.

3. Results and Discussion

3.1. Single-crystal X-ray crystallography

Crystal data, data collection and structure refinement details of the five compounds are summarized in **Table 1**.

Table 1 Crystallographic data and structure refinements summary for four products

Compounds	**1**	**2**	**3**	**4**	**6**
Chemical formula	$C_{18}H_{16}N_2O_6$	$C_{10}H_8N_2O_4$	$C_{10}H_{10}N_2O_5$	$C_{10}H_{12}N_2O_6$	$C_5H_8NO_4$
*M*r	356.33	220.18	238.20	256.22	146.12
Crystal habit	block/colorless	block/colorless	block/colorless	block/colorless	block/colorless
Crystal system	triclinic	monoclinic	monoclinic	monoclinic	triclinic
Space group	*P -1*	*P* $2_1/n$	*P* $2_1/c$	*C 2/c*	*P -1*
a /Å	8.239(4)	6.1101(4)	6.046(4)	7.2617(7)	5.731(3)
b /Å	10.295(5)	11.6530(7)	24.896(15)	7.3552(5)	6.552(3)
c /Å	10.351(5)	7.1284(5)	7.529(5)	21.1448(17)	8.794(4)
α /°	96.549(5)	90.00	90.00	90.00	92.605(7)
β /°	107.849(6)	103.940(7)	101.202(9)	92.161(7)	96.025(6)
γ /°	103.068(6)	90.00	90.00	90.00	105.321(6)
V /Å^3	798.0 (6)	492.60(6)	1111.7(12)	1128.57(16)	315.8(3)
Z	2	2	4	4	2
*D*calc. /g·cm^{-3}	1.483	1.485	1.423	1.508	1.537
μ /mm^{-1}	0.113	0.117	0.116	0.126	0.134
T /K	298	293	298	293	293
F(000)	372	228	496	536	154
*R*int	0.0544	0.0243	0.0542	0.0400	0.0191
R_1 [$I>2\sigma(I)$]	0.0633	0.0452	0.0497	0.0642	0.0476
wR_2/reflections	0.1719/2769	0.1251/1170	0.1088/2544	0.1754/1304	0.1266/1374
S	1.025	1.030	0.917	1.045	1.029

3. 1. 1. Crystal structure of 1

As an unsaturated norcantharimide (UNCI) dimer, **1** has appeared before, [**17**] but no detailed structure information has been reported. Monomeric and packing structures of **1** are depicted in **Fig. 1**. As can be seen from the figure, the polycyclic imide skeleton has the *exo*-conformation, which is more stable than the *endo*- structure and inevitably becomes the overwhelmingly major products under thermodynamic control. [**18**, **11(c)**] As for the –CH_2-CH_2- linker, **1** prefers antigauche mode. Though the asymmetric unit contains one complete dimer, the structure adopts "approximately" C_2 point-group symmetry and the C_2 axis nearly parallel to [**4 7 -6**] direction

through the center of C9-C10 bond (perpendicular to the bond). "Approximately" means the two nearly identical halves have some differences (**Table S1**, All "**S**" numbered tables and figures are in Supporting Information). For example, the double bond length of C5=C6 is 1.300(3) Å, but that for C15=C16 is 1.304(3) Å.

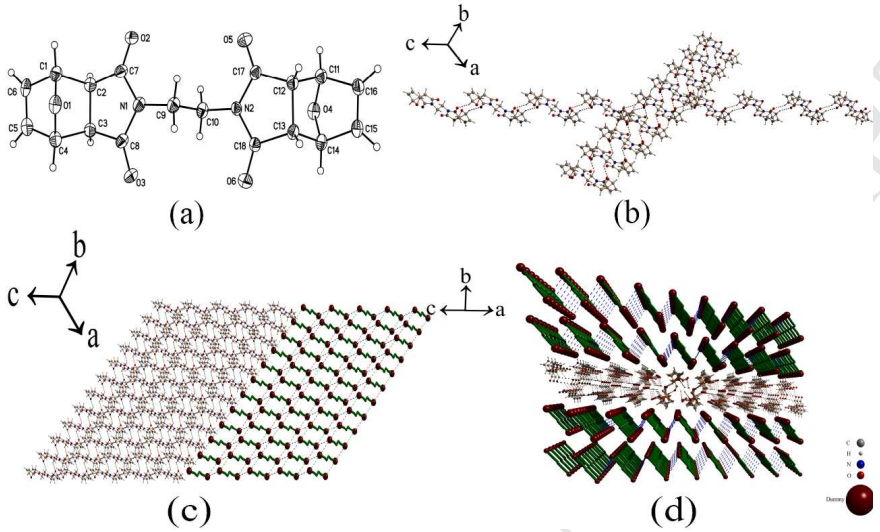

Fig. 1. (a) Atom numbered molecular structure of **1** with displacement ellipsoids for non-H atoms drawn at the 30% probability level at 298 K. **(b)** Two infinite 1D chains of **1** formed through four kinds of intermolecular C–H···O H-bonds (shown orange, green, red and blue dotted lines respectively, color figure available online), view along the **[1 1 1]** direction. The sloping chain extends along the **[-4, 3, -7]** direction and the horizontal one extends along the ***c*** axis. **(c)** 2D structure formed by intermolecular C–H···O H-bonds, view along the **[1 1 1]** direction. The right half is illustrated by the simplified structures, *i.e.* polycyclic imide skeleton except N is simplified by its center gravity (red balls at each end of the chains) and all H atoms have been omitted for clarity. **(d)** 3D structure formed by the packing of single-sheet architecture, view along the **[1 0 1]** direction. The upper two and lower two sheets are illustrated by the simplified dimers. The different objects in this figure are not drawn to scale.

In the packing structure of **1**, no valuable π-π stacking interactions can be found and the dominant force is hydrogen bonding. The geometries of hydrogen bonds are listed in **Table S2**. As can be seen, four kinds of intermolecular C–H…O hydrogen bonds are present and they adopt C_2 point-group symmetry too. Hydrogen bonds C4—H4···O5$^{(x, y, z+1)}$ and C11—H11···O3$^{(x, y, z-1)}$ are symmetry related (both involve carbonyl O), and both of them can link the dimer units into the same 1D chains, spread along the crystallographic ***c*** axis (**Fig. 1b**). Similarly, hydrogen bonds C9—H9A···O1$^{(-x+1, -y+2, -z+2)}$ and C10—H9B···O4$^{(-x, -y+2, -z+1)}$ are symmetry related (both involve bridge O), but they must work together to link the dimer units into 1D chains, which extend along the **[-4, 3, -7]** direction (**Fig. 1b**). If all the four H-bonds are considered, two-dimensional supramolecular layers with rhombic meshes are formed (**Fig. 1c**), which are aligned parallel to the ***ac***-plane of the crystal (**Fig. 1d**). Packing of these layers in the crystal is stabilized only by van der Waals forces.

3. 1. 2. Crystal structure of 2

Compound **2** is a well known bismaleimide and its spectra and physical data have been

reported in the literatures [**19**], however its single-crystal structure has not been unambiguously determined till now.

Dimer **2** is not as complicated as **1** in symmetry. The structure of **2** adopts C_i point group symmetry with an inversion center between the center two C atoms (C5-C5A). The asymmetric unit contains only one half-molecule, so the two halves are really identical. As can be seen from **Fig. 2(a)**, dimer **2** maintains the same antigauche conformation as that in dimer **1**.

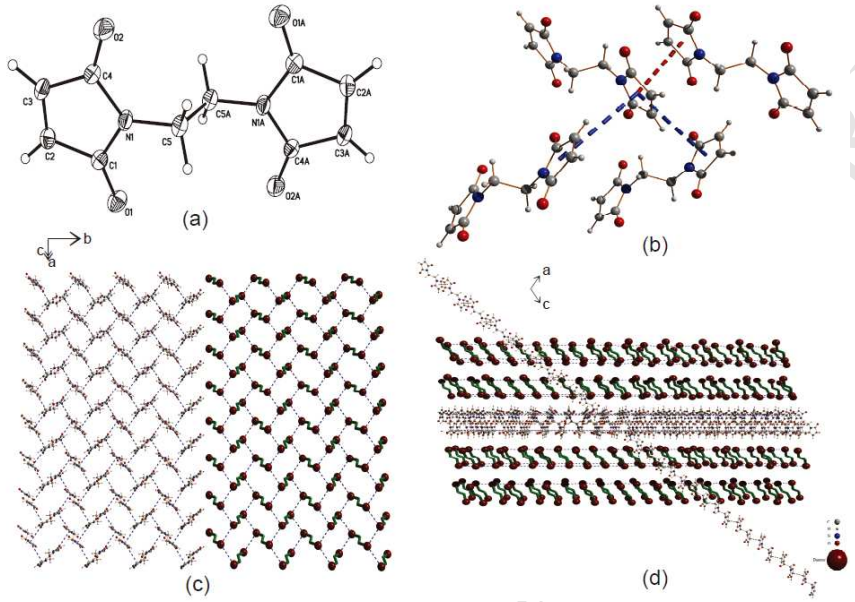

Fig. 2. (a) Atom numbered molecular structure of **2** with displacement ellipsoids for non-H atoms drawn at the 30% probability level at 293 K. Symmetry code of A: $-x+1, -y, -z$. **(b)** Two kinds of π-π interactions, shown with red and blue dotted lines, respectively. The red one corresponds to Cg1→Cg1 $^{\#1}$, #1: *-x*, 1-*y*, *-z*, *d*=3.5519(11) Å. The blue dotted lines correspond to Cg1→Cg1 $^{\#2}$, #2: 1/2+*x*, 1/2-*y*, 1/2+*z*, *d*=5.1775(12) Å. **(c)** Two-dimensional structure formed by the second kind of π-π interactions (shown blue dotted lines), view perpendicular to the spreading plane, *i.e.* the crystallographic **(2 0 3)** plane. The right half is illustrated by the simplified structures, *i.e.* imide ring except N is simplified by its center gravity (red balls at each end of the chains) and all H atoms have been omitted for clarity. **(d)** Three-dimensional structure formed by two kinds of π-π interactions, view along the ***b*** axis. The sloping chain extending along the ***c*** axis is formed by the first kind of π-π interactions and the horizontal layers spreading along the **(2 0 3)** plane are formed by the second kind of π-π interactions. Only five layers are present and their adjacent layers have been omitted for clarity. The upper two and lower two layers are illustrated by the simplified structures.

Contrary to that in dimer **1**, no classical H-bonds were found and only π-π stacking interactions occur in the packing structure of **2**. The geometries of two kinds of π, π –interactions are listed in **Table S4** and the schematic illustration is shown in **Fig. 2(b)**. The first kind of π, π –interactions (red dotted line) link dimer **2** into 1D chains stretching along the ***c*** axis (**Fig. 2(d)**), while the second kind of π, π –interactions (blue dotted lines) link dimer **2** into 2D layers parallel to the crystallographic (**2 0 3**) plane (**Fig. 2(c)**). The latter planes are further pillared by the former chains to generate 3D networks (**Fig. 2(d)**).

3. 1. 3. Crystal structure of 3

Compound **3** is new both in molecule structure and in crystal structure. It's the result of partly hydrolysis of dimer **2**, *i.e.* only one maleimide ring in dimer **2** is converted into 4-oxobutenoic acid. The O–H distances are 1.09 (3) Å and 1.39 (3) Å, respectively, and it appears that the O, H, O atoms are nearly collinear (178°) (**Fig. 3(a)**). This intra-molecular hydrogen bond O2···H1—O3 (O···O 2.472 (2) Å) gives a 7-membered ring with an average r.m.s. deviation from planarity of 0.0764 Å. The 5-membered maleimide ring has a relatively better coplanarity with an average r.m.s. deviation only 0.0039 Å. The dihedral angle between the two planes is 54.5°. As for the -C5-C6- single bond linker between these two planes, **3** prefers gauche conformation. As mentioned above, both dimers **1** and **2** adopt antigauche mode. In fact, compound **4** also crystallizes in antigauche mode. Then why only **3** prefers gauche conformation? Results from DFT calculations about different conformations of **2**, **3** and **4** prove that their gauche modes are more stable than corresponding antigauche modes (**Fig. S9** and **Table S6**). But the energy separations are very small, for example, the energy difference between the gauche and antigauche conformations of **3** is around 0.45 kcal/mol in gas phase and only 0.20 kcal/mol in solution. So the mode which facilitates intermolecular hydrogen bonding and π-π stacking in the condensed phase will become the end conformation, though the end conformation may have slightly higher energy. That's the case in **2** and **4**.

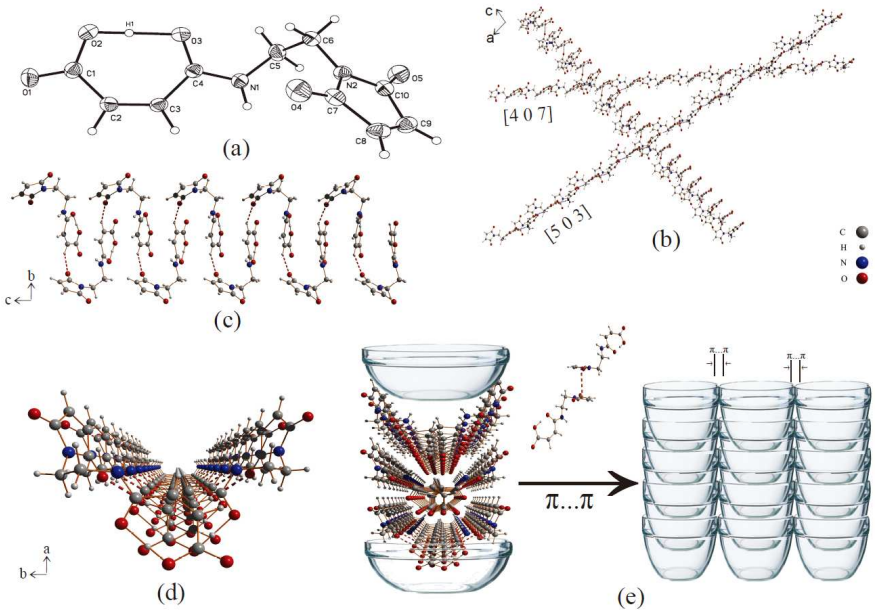

Fig. 3. (a) Atom numbered molecular structure of **3** with displacement ellipsoids for non-H atoms drawn at the 30% probability level at 298 K. **(b)** Three types of 1D chains formed through three kinds of intermolecular H-bonds (N1—H4···O1^{i}, i: *x*+1, −*y*+1/2, *z*+1/2; C2—H2···O4^{ii}, ii: *x*, −*y*+1/2, *z*−1/2; C8—H9···O3^{iii}, iii: *x*+1, *y*, *z*+1, shown blue, red and green dotted lines respectively), view along the ***b*** axis. The horizontal chain extends along the [**4 0 7**] direction and the sloping two chains extend along the ***c*** axis and the [**5 0 3**] direction. **(c)** One interesting 1D bowl-like zigzag chain, view perpendicular to the extending direction, *i.e.* ***c*** axis. **(d)** End-on view of the aforementioned 1D bowl-like zigzag chain, view along the extending direction. **(e)** The 2D layer structure formed by H-bonds further stack into 3D network through π-π interactions (orange dotted lines between two molecules above the arrow). Among the five superimposed end-on-view chains illustrating the 2D layer, the upper one and the lower one are simplified into bowls. At last, all these bowl-like zigzag chains are simplified into bowls

in the 3D network.

In compound **3**, there are three kinds of intermolecular hydrogen bonds (**Table S7**), which join molecules into three kinds of infinite chains running in the [**5 0 3**], [**4 0 7**] and ***c*** directions, respectively (**Fig. 3(b)**). All these chains are parallel to the ***ac*** plane, so their crosslinking leads to the formation of layers lying on the ***ac*** plane. These layers are overlapped in the ***b***-direction to form 3D network. It's worthy to note that the zigzag chains along the ***c*** direction exhibit an unusual bowl shape (**Figs. 3(c)** and **3(d)**). So an interesting packing pattern (**Fig. 3(e)**) is obtained due to the involvement of intermolecular hydrogen bonding and the occurrence of the π-π stacking interactions (**Table S8**).

3. 1. 4. Crystal structure of 4

Like **2**, dimer **4** (with C_i point group symmetry) resides on a crystallographically imposed inversion center and the asymmetric unit contains only one half-molecule. As shown in **Fig. 4(a)**, the central ethylene group exhibits an antigauche conformation and the symmetry-related two 4-oxobutenoic acid groups have linear O-H···O hydrogen bonds (178°).

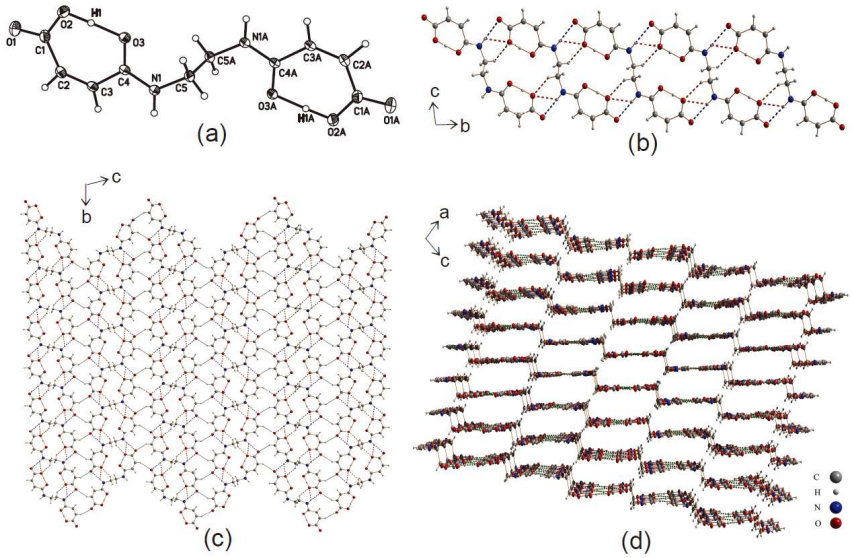

Fig. 4. (a) Atom numbered molecular structure of **4** with displacement ellipsoids for non-H atoms drawn at the 30% probability level at 293 K. Symmetry code of A: $-x+2, -y+2, -z+1$. **(b)** Three kinds of intermolecular H-bonds (N1—H4···O1^{i}, N1—H4···O2^{i}, C5—H6···O2^{i}, i: $x, y+1, z$, shown with blue, red and orange dotted lines respectively) link the dimers into 1D chains extending along the ***b*** axis. **(c)** 2D layer network formed by the fourth kind of intermolecular H-bonds (C2—H2···O1^{ii}, ii: $-x+3/2, y+1/2, -z+1/2$, shown green dotted lines), lying the crystallographic (**17 0 -17**) plane, view along the ***a*** axis. **(d)** 3D structure formed by the packing of 2D layers, view along the ***b*** axis.

Four types of intermolecular N−H···O and C−H···O hydrogen bonds are found in the packing structure (**Table S10**). Three of them link the dimers into 1D chains extending along the ***b*** axis (**Fig. 4(b)**) and the other one link adjacent dimers into 2D layers parallel to the crystallographic (**17 0 -17**) plane (**Fig. 4(c)**). No hydrogen bonds or π-π interactions can be found between these 2D hydrogen-bonded networks. So the 2D layers stack along the direction of the ***a***-axis into 3D networks mainly through Van der Waals forces (**Fig. 4(d)**).

3. 1. 5. Crystal structure of 6

Though the X-ray crystal structure of **6** was known [**20**], its H-bonding pattern was not described clearly in the original report.

Molecular and packing structures of **6** are depicted in **Fig. 5**. Relevant bond distances and angles are given in **Table S11**, and the geometries of hydrogen bonds are listed in **Table S12**. X-ray structural analysis reveals that the asymmetric unit comprises of a deprotonated maleate anion, and one half protonated ethylenediammonium dication located in an inversion center (**Fig. 5(a)**). Hydrogen transfer from maleate acid to ethylenediamine was observed after the hydrolysis of dimer **4**, yielding three oppositely charged spheres. Our DFT calculations prove that the proton transfer is inevitable in implicit solvent model of CPCM, *i.e.* no stable structure including neutral fragments (maleate acid and ethylenediamine) can be obtained in ethanol solution. They can coexist only in gas phase, with around 39.8 kcal/mol higher energy than that of ionic fragments (two deprotonated maleate anions and one protonated ethylenediammonium dication), and the former will always be optimized into the latter in ethanol solution. These ionic fragments were held together by electrostatic interactions as well as hydrogen bond (N1—H6···O4). Linear O-H···O hydrogen bonds still occur in the maleate anion, but less linear with the angle only 173° instead of aforementioned 178° in **3** and **4**.

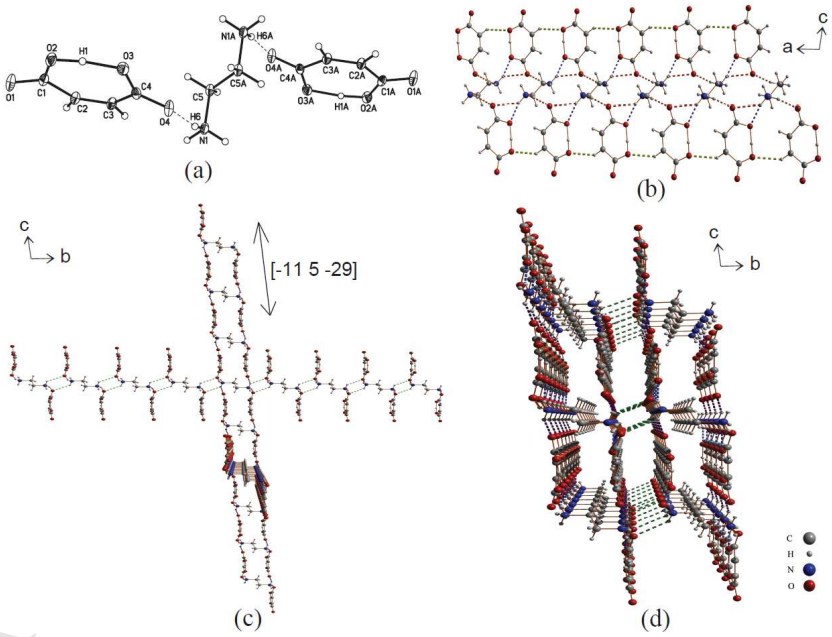

Fig. 5. (a) Atom numbered molecular structure of **6** with displacement ellipsoids for non-H atoms drawn at the 30% probability level at 293 K. Symmetry code of A: $-x+2, -y+2, -z+1$. **(b)** Three kinds of intermolecular H-bonds (N1—H7···O3^{i}, N1—H7···O4^{i}, C2—H2···O2^{i}, i: $x-1, y, z$, shown with blue, red and yellow dotted lines respectively) link the dimers into 1D chains extending along the ***a*** axis. **(c)** Three kinds of 1D chains extending along different directions: the horizontal chain along the ***b*** axis (link by N1—H8···O4^{ii}, ii: $-x+1, -y+1, -z$), the sloping chain along the **[-11 5 -29]** direction (link by N1—H8···O1^{iii}, iii: $x-1, y, z-1$) and the end-on view of the aforementioned 1D chain along the ***a*** axis. **(d)** The aforementioned three kinds of chains weave with each other leading to the formation of 3D structure, view along the ***a*** axis.

In the packing structure of **6**, there are five kinds of intermolecular N−H···O and C−H···O hydrogen bonds (**Table S12**), each of which can link the compound into 1D chains. Three types of hydrogen bonds involving the molecules with the symmetry code "*x*−1, *y*, *z*" coexist in the same kind of 1D chains extending along the ***a*** axis (**Fig. 5(b)**), which look like chairs from the point of end-on view, *i.e.* along the ***a*** axis (**Figs. 5(c)** and **5(d)**). The other two types of intermolecular hydrogen bonds join molecules into two kinds of 1D chains running in the [**-11 5 -29**] and ***b*** directions, respectively (**Fig. 5(c)**). At last, these 1D chains with different orientations weave with each other leading to the formation of 3D network with microporous structure.

In summary, dimer **1** possesses axial symmetry and dimers **2**, **4**, **6** possess central symmetry, they all exhibit antigauche conformation, while **3** prefers slightly more stable gauche mode. All five compounds crystallize in the centrosymmetric space group and the dominating forces are hydrogen bonding as well as π-π stacking interactions, which link the molecules into interesting 1D, 2D and 3D networks.

3.2. Proposed Mechanisms of Hydrolysis

The hydrolytic degradation pathways of **2** without or with water catalysis were proposed based on the identified crystal structures of these degradation products and shown in **Scheme 2**. It can be seen that all degradation reactions induced by water occur in the C–N bonds, which are broken step by step until the elimination of the last O=C–N bond. Nevertheless, product **5** is hard to be obtained experimentally, which means the activation energy of the last step may be the lowest one. The chemical elucidation of the proposed hydrolytic degradation pathways need to be proved further in future study.

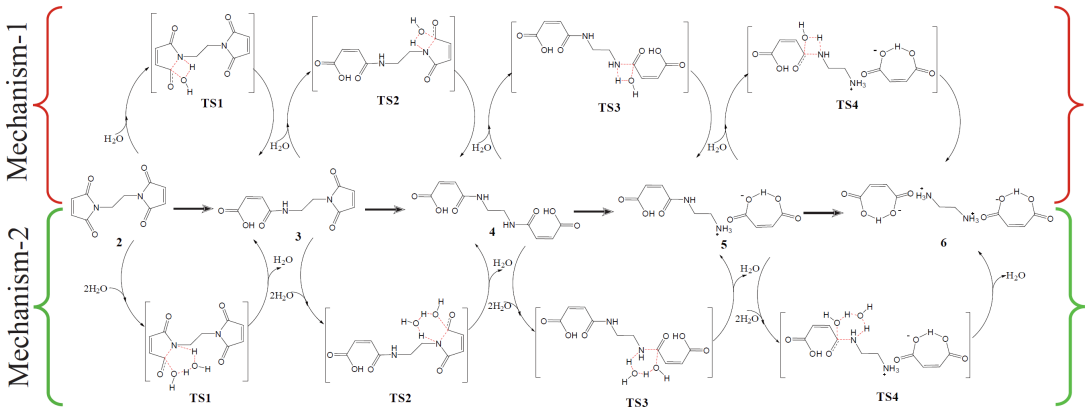

Scheme 2. Proposed mechanisms without or with water catalysis of continual four-step hydrolytic degradation reaction of N, N'-ethylenedimaleimide (dimer **2**).

In **Mechanism-1**, TS structures form tetragonal rings due to the attack of one water molecule, while the TS structures in **Mechanism-2** produce stable hexagonal rings in the presence of two water molecules. So it can be deduced that the activation energies in **Mechanism-2** should be lower than that in **Mechanism-1**, *i.e.* one water molecule plays role of a catalyst. Obviously such speculation needs to be investigated further.

4. Conclusions

Five single-crystal structures related with the same reaction have been investigated. **1**, **2**, **4**, **6** are dimers linked by $–CH_2-CH_2-$ group and only **3** has non-symmetry related skeleton, which is the product of partly hydrolysis of dimer **2**. Though all four dimers exhibit antigauche conformations, gauche modes are in fact more stable than corresponding antigauche modes, which have been proved by DFT calculations as well as the crystal structure of **3**. It is hydrogen bonding and π-π stacking interactions in the condensed phases that drive these dimers into antigauche modes. Still because of hydrogen bonding and π-π stacking interactions, the molecules form different kinds of packing structures, which have been investigated and graphically represented. Among these five crystal structures, the most interesting one is that of **3**, in which one kind of intermolecular hydrogen bonds link molecules into bowl shape zigzag chains and these "bowls" are further overlapped into 2D and 3D networks by other kinds of intermolecular hydrogen bonding and π-π stacking interactions.

It should be mentioned that what set these molecules apart are not only their crystal structures but also their experimental evidence in the investigation of hydrolytic degradation mechanism. Two reaction pathways have been proposed. **Mechanism-1** involves only one H_2O molecule, which acts as reactant; **Mechanism-2** involves two H_2O molecules, which act as reactant as well as catalyst. The detailed chemistry needs to be investigated further.

5. Acknowledgments

The authors are thankful to the Science & Technology Development Projects of Shandong Province in China (No. 2011GGX10706 and 2012GGX10702) and the National Natural Science Foundation of PR China (NSFC, No. 21103100) for financial support. Generous support in computing resources from the National Supercomputer Center in Jinan, China, is greatly appreciated.

Supplementary Material

Supplementary Information available: **Tables S1 – S26**, **Figures S1 - S9** mentioned in the text. Crystallographic information files of five compounds. CCDC < 1446298, 1454849, 1454850, 1454851, and 1454852> contains the supplementary crystallographic data for < **1, 2, 3, 4** and **6** >. These data can be obtained free of charge from The Cambridge Crystallographic Data Centre via http://www.ccdc.cam.ac.uk/data_request/cif , or from the Cambridge Crystallographic Data Centre, 12 Union Road, Cambridge CB2 1EZ, UK; fax: (+44) 1223-336-033; or e-mail: deposit@ccdc.cam.ac.uk.

References and notes

[1] V. Ondruš, L. Fišera, V. Bradac, ARKIVOC, v (2001) 60-67.

[2] V. Rao, S. Navath, M. Kottur, J. R. McElhanon, D. V. McGrath, *Tetrahedron Lett.* 54 (2013) 5011–5013.

[3] P. D. Senter, E. L. Sievers, *Nat. Biotechnol.* 30 (2012) 631–637.

[4] P. F. Peddi, S. A. Hurvitz, *Future Oncol.* 9 (2013) 319–326.

[5] R. P. Lyon, J. R. Setter, T. D. Bovee, S. O. Doronina, J. H. Hunter, M. E Anderson, C. L. Balasubramanian, S. M. Duniho, C. I. Leiske, F. Li, P. D. Senter, *Nat. Biotechnol.* 32 (2014) 1059-1062.

[6] (a) S. D. Fontaine, R. Reid, L. Robinson, G. W. Ashley, D. V. Santi, *Bioconjugate Chem.* 26 (2015) 145–152; (b) S. C. Alley, D. R. Benjamin, S. C. Jeffrey, N. M. Okeley, D. L. Meyer, R. J. Sanderson, P. D. Senter, *Bioconjug. Chem.* 19 (2008) 759–765; (c) B. Q. Shen, K. Xu, L. Liu, H. Raab, S. Bhakta, M. Kenrick, K. L. Parsons-Reponte, J. Tien, S. F. Yu, E. Mai, D. Li, J. Tibbitts, J. Baudys, O. M. Saad, S. J. Scales, P. J. McDonald, P. E. Hass, C. Eigenbrot, T. Nguyen, W. A. Solis, R. N. Fuji, K. M. Flagella, D. Patel, S. D. Spencer, L. A. Khawli, A. Ebens, W. L. Wong, R. Vandlen, S. Kaur, M. X. Sliwkowski, R. H. Scheller, P. Polakis, J. R. Junutula, *Nat. Biotechnol.* 30 (2012) 184–189; (d) V. L. Chudasama, F. S. Stark, J. M. Harrold, J. Tibbitts, S. R. Girish, M. Gupta, N. Frey, D. E. Mager, *Clin. Pharmacol. Ther.* 92 (2012) 520–527.

[7] (a) C. P. Ryan, M. E. B. Smith, F. F. Schumacher, D. Grohmann, D. Papaioannou, G. Waksman, F. Werner, J. R. Baker, S. Caddick, *Chem. Commun. (Camb.)* 47 (2011) 5452–5454; (b) P. Knight, *Biochem. J.* 179 (1979) 191–197.

[8] G. Dahlgren, N. L. Simmerman, *J . Phys. Chem.* 69 (1965) 3626-3630.

[9] A. J. Kirby, P. W. Lancaster, *J. Chem. Soc., Perkin Trans.* 2 (1972) 1206-1214;

[10] S. Matsui, H. Aida, *J. Chem. Soc., Perkin Trans. 2* 12 (1978) 1277-1280.

[11] (a) S. Baggio, A. Barriola, P. K. de Perazzo, *J. Chem. Soc., Perkin Trans. 2* (1972) 934-937; (b) B. M. Ramirez, G. D. de Delgado, W. O. Velasquez, G. M. Perdomo, *Z. Kristallogr.-New Crystal Structures,* 213 (1998) 197-198; (c) Y. W. Goh, B. R. Pool, J. M. White, *J .Org. Chem.* 73 (2008) 151-156.

[12] M. Viswanathan, *Asian J. Chem*. 17 (2005) 2611-2615.

[13] G. M. Sheldrick, SADABS, Bruker AXS Inc., Madison, Wisconsin, USA, 2004.

[14] G. M. Sheldrick, *Acta Crystallogr, Sect. A*, 64 (2008) 112-122.

[15] Bruker APEX II (version 2.0-1), SAINT (version 7.23A), XPREP (version 2005/2), SHELXTL (version 6.1). Bruker AXS Inc., Madison, Wisconsin, USA, 2005.

[16] K. Brandenburg, H. Putz, DIAMOND. Crystal Impact GbR, Bonn, Germany, 2005.

[17] (a) L. P. Deng, Z. Yong, W. F. Tao, J. F. Shen, W. Wang, *J. Heterocyclic Chem.* 48 (2011) 158-161; (b) V. Rao, S. Navath, M. Kottur, J. R. McElhanon, D. V. McGrath, *Tetrahedron Lett*, 54 (2013) 5011-5013.

[18] (a) M. W. Lee, W. C. Herndon, *J. Org. Chem.* 43 (1978) 518-518; (b) P. X. Iten, A. A. Hofmann, C. H. Eugster, *Helv. Chim. Acta* 62 (1979) 2202-2210 and litt. therein.

[19] (a) Y. H. Kim, W. E. Stites, 47 (2008), 8804–8814; (b) D. Habibi, O. Marvi, *ARKIVOC*, xiii (2006) 8-15; (c) R. Tona, R. Häner, *Mol. BioSyst.*, 1 (2005) 93-98; (d) A. A. Kumar, K. Dinakaran, M. Alagar, *J. Appl. Polym. Sci.*, 89 (2003) 3808-3817; (e) I. M. Brown, T. C. Sandreczki, *Macromolecules*, 23 (1990) 4918–4924; (f) P. Kovacic, R. W. Hein, *J. Am. Chem. Soc.* 81 (1959) 1187–1190.

[20] J. C. Barnes, T. J. R. Weakley, *Acta Cryst.* C53 (1997) IUC9700018.

Keywords: N,N'-ethylenedimaleimide, crystal structure, key intermediates, hydrolysis mechanism

Highlights

1) Five single-crystal structures have been investigated; molecular conformations and weak interactions have been analyzed.

2) The hydrolytic degradation mechanisms of N,N'-ethylenedimaleimide without or with water catalysis have been proposed.